Real-Time IoT Solution to Monitor and Control dMVHR Units in Real-Life Environment

Ferenc Tolvaly-Roşca[1], Gusztáv Fekete[2*], István Bíró[3], Albert-Zsombor Fekete[4], Zoltán Forgó[1]

[1]Department of Mechanical Engineering, Faculty of Technical and Human Sciences, Sapientia Hungarian University of Transylvania, Sighișoarei road no. 2, 540485 Târgu Mureş, Romania; zforgo@ms.sapientia.ro, tferi@ms.sapientia.ro

[2]Department of Material Science and Technology, AUDI Hungária Faculty of Vehicle Engineering, Széchenyi István University, Egyetem tér 1, 9026 Győr, Hungary; fekete.gusztav@sze.hu

[3]Institute of Technology, Faculty of Engineering, University of Szeged, Mars tér 7, 6724 Szeged, Hungary; biro-i@mk.u-szeged.hu

[4]Department of Electrical Engineering, Faculty of Technical and Human Sciences, Sapientia Hungarian University of Transylvania, Sighișoarei road no. 2, 540485 Târgu Mureş, Romania; zsombor.feketefazs@ms.sapientia.ro

Abstract: This paper presents an up-and-running control system, using IoT hardware, for multiple decentralized mechanical ventilation with heat recovery (dMVHR) units to enhance the overall performance of heat exchangers and the air quality of a real-life environment. The implemented control and monitoring system is able to measure the thermal efficiency of the complete ventilation system under real working conditions. Fan speed is automated based on the measured CO_{2eq} levels in the bedrooms of the building, however, manual control is also possible. Temperature, relative humidity and CO_{2eq} levels can be monitored live on the user's smart device, while data can be exported through Google cloud system. Data values can be stored and accessed any time by legit users. The thermal efficiency of the individual units and the whole ventilation system was investigated and experimentally verified under real-life conditions, using the implemented centralized control and monitoring system.

Keywords: decentralized mechanical ventilation with heat exchanger; IoT, distributed embedded system; data acquisition; environmental sensors

1 Introduction

Energy consumption for HVAC systems (heating, ventilation, and air conditioning) of buildings represents not only 40% of the European Union's total energy demand but also for the half of the world [1]. It is estimated that HVAC system use, in general, 40–60% of a building's energy needs [1, 2].

Heat loss of building can be reduced by specific construction technologies, or subsequent to the construction stage by insulating and sealing the building envelope. However, sealing and insulating a building has consequences in the form of reduced air exchange, which may lead to severe deterioration of indoor air quality (IAQ). To improve air quality inside the buildings, mechanical ventilation is used, which leads to great heat loss with the exhaust air. To reduce energy consumption, heat energy contained in the exhaust air is partially recovered. The recovery process efficiency depends on the airflow (more airflow means less efficiency) and on the temperature difference between outside and inside. To perform an efficient recovery process, Mechanical Ventilation with Heat Recovery (MVHR) and Energy Recovery Ventilation (ERV) systems are used. It must be mentioned that an MVHR system can be centralized or decentralized (dMVHR). Typically, dMVHR systems can achieve a thermal efficiency of 90-95% [3, 4, 5, 7, 8] and due to their relative simplicity, they are used in a large number of buildings across Europe [5, 6].

It should be noted that dMVHR systems use individual units, which can be controlled separately but also with a central control system. The unit's flow direction and flow rate can be regulated by controlling the fan's rotating direction and spindle. This control can assure an optimal IAQ and noise control for each individual room. A typical dMVHR unit includes a heat exchanger, a fan, and a filter as they are seen on Figure 1.

In recent years, smart home automation (fused with IoT devices) has spread to improve not only the energy efficiency of the building (by adjusting the ventilation to the actual occupancy of the building) but the IAQ as well, enhanced by regulating the air flow in different areas of the building [10, 11, 12, 13, 14]. These systems contribute significantly to the increasing energy efficiency [13, 14] and living conditions of buildings without compromising comfort [15, 16, 17].

In the presented paper our aim is threefold. First, we present an automated IoT solution, which controls 4 dMVHR units in order to maintain and monitor temperature (T), realtive humidity (RH) and carbondioxide (CO_2) levels in an actual building. Second, we present a simple & stable application to acquire and analyze data regarding IAQ parameters for immediate or postponed analysis. Third, we aim to create such data, which is adequate to investigate and compare the dMVHR units operating parameters with the unit's advertised parameters.

From these results the real efficiency of the system can be estimated, together with the capability of the IoT solution in monitoring real time parameters.

2 Materials and Methods

2.1 dMHVR Units and their Application on an Actual Building

The automation project uses a previously installed Aerauliqua Quantum HR150 MHVR system (Figure 1, main parameters in Table 1), built with 2 + 2 units (U1.1, U1.2, U2.1, U2.2) together with their mechanical switches, which can short S1, S2, S3 channels/connections. The model is a decentralized type of MVHR, with alternative flow direction.

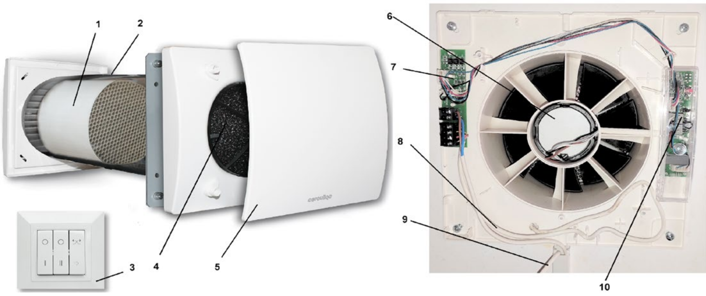

Figure 1

Components of a decentralized MVHR unit (Aerauliqua HR150) [9]: 1 - Ceramic heat exchanger; 2 – telescopic duct; 3 – simple mechanical switch; 4 – Dust filter; 5 – Unit cover; 6 – Fan with brushless DC motor; 7 – Power unit; 8 – Cable linking with the pair MVHR unit; 9 – Sensor's cable; 10 – Individual control unit

Table 1

Contains the result of comparing in pairs with the final result

Parameter	Units	Value
Thermal efficiency of heat	%	74
SEC class	-	A
Maximum flow rate @ 0 Pa	m^3/h	60
Electric power input	W	3.8
Control typology	-	Manual control (no
Type of drive	-	Multi-speed drive
Specific power input (SPI)	$W/m^3/h$	0,054
Air-flow at different speed	m^3/h	60/40/20
Power consumption at different	W	3.8 / 2.3 /1.4
AEC - average climates	kWh	0.7
Sound pres. @ 3m at different	dB(A)	26/18/10
Thermal efficiency	%	70/74,3/82
Ambient temperature max.	°C	-20°C ÷ +50°C

According to manual of the unit [9], it is intended to be used in continuous mode since power consumption is very low (4 units x 1.4 Wh x 24 h = 134.4Wh in a day). The units lack any automation or measuring capabilities, however, this feature offers a variety of possible improvements made by a user with automation knowledge.

The building where the dMVHR units are installed, is a two-story house. The external walls have 50 cm thickness, and the building has a complete inner surface of 103 m^2, with an approximate inner volume of 250 m^3.

Ventilation units are placed as depicted in Figure 2. Namely, two on the ground floor and two on the 1st floor. These units are indicated by red and green colors and noted by U1.1, U1.2 and U2.1 and U2.2.

Figure 2

The dMHRV units in the building (ventilation columns: green – column 1, red - column 2)

The dMVHR units with alternative airflow work only as a pair since in a closed space a single ventilation unit cannot circulate air. It must be noted that the two ventilation systems work independently on both floors and each unit has its own individual power and control electronics board (Figure 2).

The two floors communicate through a staircase with 1 m width and 2.2 m height. The staircase has no doors. The bedrooms have doors with a 2 cm gap under the 1 m wide doors. This means that the door represents an approximate 200 cm^2 cross - section. In Figure 2 the non-used, non-ventilated rooms are crosshatched. As depicted in the Figure 2, the total ventilated surface is approximately 70 m^2 with a ventilated volume of 180 m^3.

With regard to air quality, the international health normative for IAQ requires not less than 25-30 m^3/h per person. According to this normative, the presented building needs a minimum of 0.3 x 180 = 54 m^3/h continuous airflow volume. According to the unit's specification 2 x 20 m^3/h volumetric flow rate can be achieved at the lowest fan speed. As there are two pairs, working in parallel, their total volumetric rate is 40 m^3/h. To meet the neccesary 54 m^3/h criteria, the units shall only use higher speed until the desired CO_2 or RH levels are achieved.

2.2 Topology of the Control System

Beside the feasibility of maintaining adequate IAQ level, price is also an important factor in the design of a control system. It must be noted that the price of a centralized MVHR for the presented building (with the installation of the duct system as well) starts from 4000 €. Commercial dMVHR units, featuring a wireless connection between two or more units, a centralized remote control of fan speed, without measuring temperatures, relative humidity or CO_2 levels and featuring a time dependent automation of fan speed, costs around 800 €/unit plus the automation cost of 300 €.

As a cost-effective solution, we proposed a distributed data acquisition and control system (Figure 3) for monitoring key environmental parameters, such as room temperature, relative humidity and CO_2 levels. The developed system uses a centralized or so-called star topology for interconnecting the system`s unit. This is divided into two categories: central control unit and hub units. The hub units, regardless of their deployment, present identical buildup, and their distinction is based on a unique identification number ranging from 1 to 4, in function of the room in which they are installed.

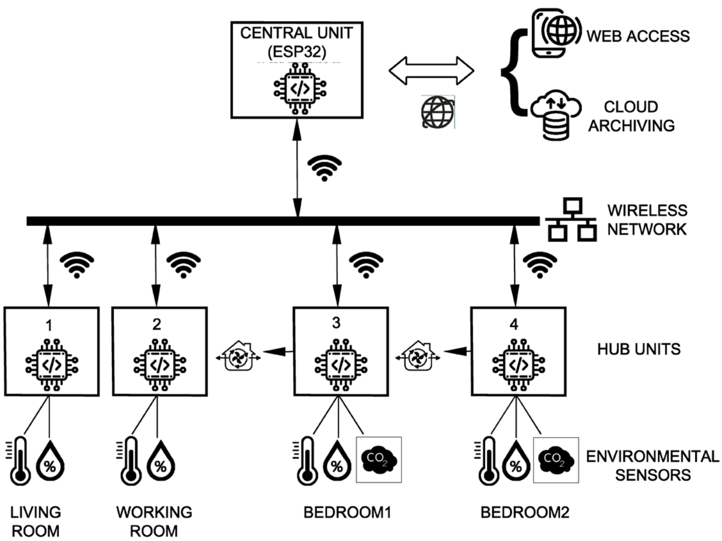

Figure 3

The proposed distributed data acquisition system

2.3 Sensors and Control

In order to maintain good health in the living habitat, it is essential to ensure the reliability of the sensor data. This can be achieved by applying hub units, which acquire the environmental measurements and a center control unit [18], which carries out the interpretation and decision making process (Figure 4).

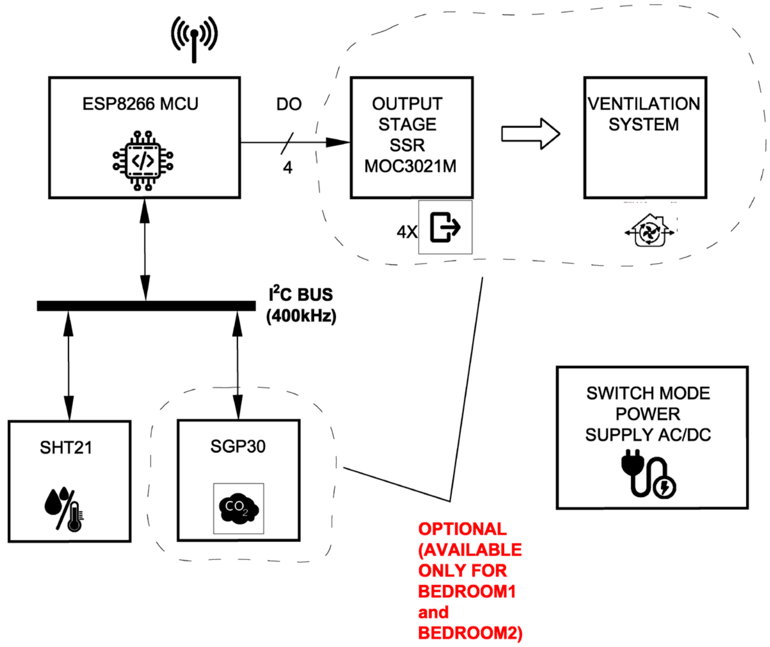

Figure 4
Hardware design of the hub units

In this system, the hub units act as I/O extension modules, incorporating wireless network connectivity, environmental sensors and solid-state output stages for controlling the ventilation system. The hubs are built around the Espressif ESP8266 32-bit microcontroller, a cost-effective and highly integrated Wi-Fi MCU designed for IoT applications. With plenty of hardware and software resources, the MCU unit focuses on executing the following main tasks: establishing and maintaining a stable connection with the habitats existing network via Wi-Fi, receiving and transmitting encoded UDP packets, data exchange with digital environmental sensors, as well as interpreting and executing control commands regarding the fan speed of the ventilation system.

The solid-state output stage is designed around four MOC3021M type opto-triacs, one for each fan speed selection input and one for the mode selection. By default, the ventilation system is equipped with a manual switch cluster, enabling the end user to manually select the desired fan speed (1-3) and operating mode (normal or alternating mode). As for the hardware modification, relays were replaced by solid-state switching devices. This alteration resulted in lesser noise emission.

For data acquisition we used two types of Sensirion environmental sensors, designed for IoT solutions. For temperature and relative humidity measurements each of the hub units incorporate an SHT21 digital sensor [19], whilst for CO_2 measurements an SGP30 multi-gas (TVOC and CO_2eq) sensor [20] is used. Both sensors are pre-calibrated and designed for indoor use. In addition, they offer good price-performance ratio. The main parameters are presented in Table 2.

Table 2

Enviromental sensor specifications

Sensor	**SHT21**		**SGP30**
Data type	Temperature	Humidity	CO_2
Sensor type/sensing element	bipolar junction transistor-based silicon bandgap	capacitive	metal-oxide
Operating range	-40 to 125 °C	0 to 100	400 ppm to 60000
Resolution	14 bit / 0.01	12 bit /	400 ppm to 60000
Accuracy (typical) @ 25 ºC,	±0.3 °C	±2 to ±4	10 % of measured
Repeatability	±0.1 °C	±0.1 %	-
Response time ($T_{63\%}$) / sampling frequency	5 to 30 s	8 s	40 Hz (typical)
Interface	I^2C	I^2C	I^2C
Bus Address	0x40		0x58
Bus Speed	400 kHz		400 kHz
Supply voltage	2.1 to 3.6 V		1.62 to 1.98 V
Average current consumption	330 µA		49 mA @ 1.8V
Measuring unit	°C	%	ppm

In order to minimize heat dissipation of the sensor boards, which results in unwanted drift in the measurements, both the SHT21 and the SGP30 are powered from 3.3 V, the lowest voltage level present in the proposed hardware.

The SGP30 features a fully integrated MOX gas sensor, together with an on-chip humidity compensation to measure Total Volatile Organic Compounds (TVOC) and carbon dioxide equivalent (CO_{2eq}). Total Volatile Organic Compounds refers to the total concentration of organic chemicals which exhibits high vapor pressure at room temperature. CO_{2eq} stands for carbon dioxide equivalent, which is a metric used to measure and compare the emissions of various greenhouse gases, including carbon dioxide (CO_2), methane (CH_4), nitrous oxide (N_2O), and fluorinated gases. In case of the SGP30 sensor the CO_{2eq} is calculated based on H_2 concentration.

In order to benefit from the SGP30 features, an absolute humidity value must be determined. Given the relative humidity (RH) and actual temperature (T) values, the absolute humidity (dv) can be determined using the following formula [21]:

$$d_v(T, RH) = 216.7 \cdot \left[\frac{\frac{RH}{100\%} \cdot 6.112 \cdot exp\left(\frac{17.62 \cdot T}{243.12+T}\right)}{273.15+T}\right]\left[\frac{g}{m^3}\right] \tag{1}$$

The obtained value is used for the onboard humidity compensation algorithm until a new absolute humidity value is calculated and set, therefore, it is mandatory to actualize the absolute humidity value before initiating a new CO_{2eq} read operation.

From the software structure point of view, in every data acquisition cycle the SHT21 sensor is read first, and only after the absolute humidity value is calculated. This process is followed by the SGP30 read sequence. In order to achieve valid CO_{2eq} measurements with the chosen sensor, the baseline or background level of the quantity must be known. The SGP30 features an onboard dynamic baseline compensation algorithm, based on two baseline coefficients (one for the CO_{2eq} and one for the TVOC measurements) stored externally by the ESP8266 microcontroller. Determining the exact values assumes that the sensor is exposed to “clean” or fresh air for at least 12 hours, where the CO_{2eq} concentration level is basically 400 ppm. After the given time, the baseline values are read back from the sensor and stored in the non-volatile memory of the microcontroller.

From a hardware point of view, the center control unit is fairly simple in comparison and consists of a development board based on the Espressif ESP32 Wroom [21] dual-core microcontroller.

Being at the top level, the unit’s main task, besides network connectivity, is to manage the hub units, request periodic measurement results, execute control algorithms based on the environmental data (in our case CO_2) and provide a platform for the various IoT functionalities. The units in discussion exchange data over the traditional Wi-Fi network via UDP encoded packets.

As for the deployment of both the hub units and the central control unit, it is critical to ensure an adequate signal strength from the side of the wireless network. This information can be easily obtained by accessing the built-in signal strength data provided by the microcontrollers themselves. A stable operation can be achieved with a signal strength greater than -75 dBm.

As an electrical circuit used twenty-four hours a day, seven days a week some considerations had to be made regarding the safety, durability and reliable functioning of the units in the long-term. These include: power supply dimensioning, enclosure and wiring.

Every hub and central unit deployed is powered by a dedicated 5 V switch mode power supply with a rated current output of 3A.

2.4 Firmware

For the development of the firmware applications, we used the Arduino IDE programming environment (version 1.8.19) with the following core libraries: esp8266 (by ESP8266 Community, version 3.0.2), ESP32 (by Espressif Systems, version 1.0.6). For accessing the environmental sensors, Sodaq_SHT2x (by Kees Bakker, version 1.2.0) and Adafruit SGP30 Sensor (by Adafruit, version 2.0.0) libraries were employed, whilst for the implementation of the different IoT channels and features, embedded into the central unit and presented in detail in the following sections, the WiFi, ESPAsyncWebServer, AsyncTCP, AsyncUDP and Arduino_JSON libraries were linked. The simplified flow diagram of the embedded firmware's main tasks can be seen in Figure 5.

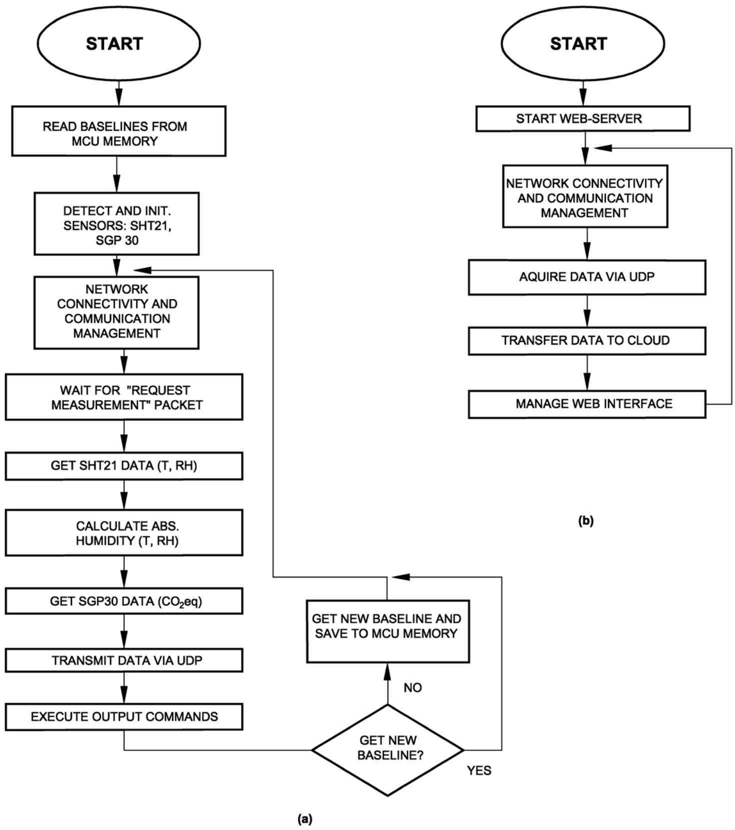

Figure 5
Simplified flow diagram of the embedded firmware's main tasks: (a) central control unit; (b) hub or data acquisition unit

The automation part of the system contains an algorithm executed on the central control unit, which controls the ventilation systems flow rate as a function of the CO_2 data.

Based on the measured CO_{2eq} levels we define and distinguish 3 intervals: normal (CO_{2eq} < 1000 ppm), medium (1000 ppm < CO_{2eq} < 1500 ppm) and high (CO_{2eq} > 1500 ppm) CO_2 concentration/health risk. Each interval corresponds to a fan speed from 1 to 3. In the case of the normal interval, the lowest or base speed is activated via the solid-state output stage. As the CO_{2eq} level increases, at medium and high CO_{2eq} concentrations speeds 2 and 3 are engaged, resulting in a higher air flow rate. The decision making control algorithm is incorporated in the central unit, the hub only acquires the data and executes the commands received from the latter. By default, the fan speed selection is set to automatic, but the system also offers a manual override possibility via the built-in web control interface or virtual Human Machine Interface (HMI).

2.5 IoT Channels and Measurements

The interconnected hubs and the central unit, presented in this paper, form an automated IoT control and data acquisition system, incorporating a web-server and cloud-based connectivity. The web interface or virtual HMI enables remote access by implementing bidirectional data flow for live data visualization and manual control possibility for the end user. Due to the automated operating mode, both IoT channels serve mostly monitoring purposes, but a logged in user has the possibility of overriding the system by switching to manual control.

The password protected control and data visualization interfaces feature dynamic data exchange between the microcontroller and the webpages in question. This implies Server-Sent Events (SSE), which enable the browser to receive dynamic data automatically via HTTP request. By using an embedded JavaS script chart stack (Highcharts), the user has access to live data (Figure 6).

The html, JavaScript, css files, and the graphic data needed to form the web pages are uploaded and stored in the SPIFFS memory of the ESP32. The asynchronous web-server enables multiple independent connections from different devices. The web interface is accessible both locally (via internal network) and globally (via Internet). The interconnected hubs and the central unit presented in this paper form an automated IoT control and data acquisition system, incorporating a web-server and cloud-based connectivity. The web interface or virtual HMI enables remote access by implementing bidirectional data flow for live data visualization and manual control possibility for the end user. Due to the automated operating mode, both IoT channels serve mostly monitoring purposes, however, a logged in user has the possibility of overriding the system by switching to manual control (Figure 9).

For long-term data archiving we decided on implementing a data transfer capability to a Google Sheet, using its IoT cloud-based services [22]. For the data transfer we opted for a direct approach in the form of a custom-made Google Script, eliminating the need for third-party services, making the data archiving more robust.

The data transfer is based on a HTTP request with a custom URL containing a unique Google Script ID and the user data. After a successful request, the deployed Google Script extracts and processes the user data from the payload and transfers it to a predefined Google Sheet.

The selected data packet includes a timestamp, room temperatures (selectable 3-90 sec sampling time from HMI), humidity values and CO_{2eq} levels (15 sec sampling times, changeable only in the source program) acquired from the 4 rooms. These form an entry in the spreadsheet, which can be downloaded and processed at any given time.

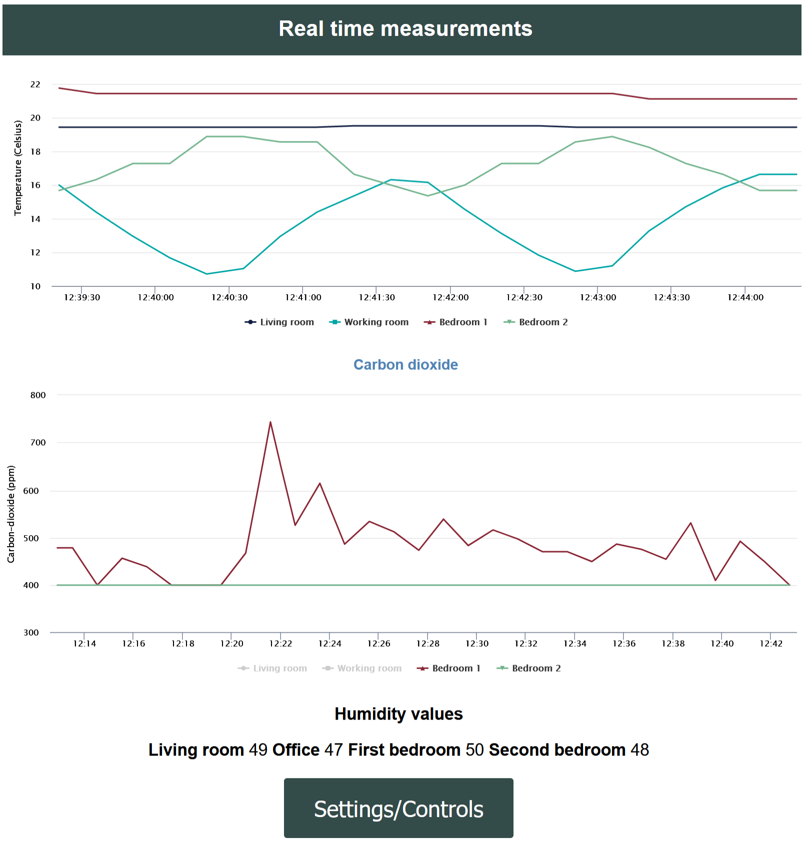

Figure 6
Live measurement of temperature and CO_{2eq} level

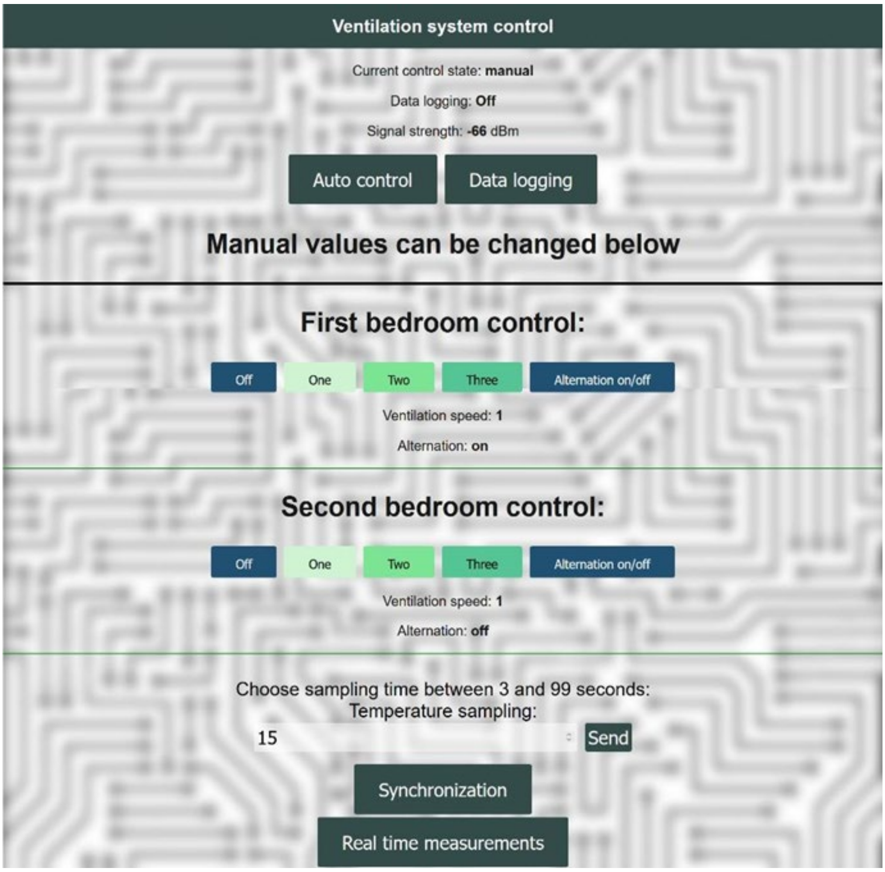

Figure 7
The ventilation system control's web interface

The live data streaming to the HMI interface works with unlimited time. It starts automatically with the firmware stars. The visualization of the data starts with the opening of the graphic interface, and stops with the close of the interface, nevertheless the data stream flows continuously.

The sampling times are set as follows: 15 seconds for $CO2_{eq}$ measuring (fixed in the firmware of the hubs) and the temperature sampling time can be set in the graphical interface between 3-99 seconds (Figure 7). 15 seconds sampling time for CO_{2eq} levels is sufficient since the change is quite slow. The sampling time for temperature measurements must be shorter if thermal efficiency is to be determined. We proposed 3 second sampling time for a 75 sec ventilation cycle- Otherwise, for general visualizations and monitoring, 15 seconds or longer time intervals can be used.

The data acquisition in the cloud (Google sheet) can be started and stopped manually from the graphical interface (Figure 7, Data logging button) for an unlimited time period.

The automation unit's practical implementation consists of two types of PCBs, which were installed in Kradex Enclosure Z12 boxes.

Finally, in order to assess the thermal efficiency of the dMVHR system, an SHT21 sensor was placed at the ducts outlet directly in the unit's air stream. For the thermal efficiency investigation, the temperatures recorded in the unit's ducts outlet and the room temperatures are monitored and analyzed. From the registered temperature values, the thermal efficiency can be determined by Equation 2, complying with DIN EN 308 standard [5]:

$$\eta_{HRC} = \frac{T_{sup,room} - T_{amb}}{T_{room} - T_{amb}} \quad (2)$$

Where: $T_{sup,\ room}$ is temperature in the outlet of the unit inside the room, T_{amb} is the temperature of the outside air and T_{room} is the temperature measured in the room. All temperatures are in [°C].

To globally evaluate the thermal efficiency of the ventilation system, the experiments must be carried out while the building's automated heating system is stopped. It must be noted that the outside temperatures ranges between -12°C to +5°C in Transylvania during the winter. The measurements must be carried out for all three fan speed to be able to determine the thermal efficiency, which is linked to the exchanged air volume flow and therefore to the fan's spindle speed.

It must be mentioned for the experiements that in prolonged use the two independent ventilation columns (U1.2 linked with U2.2 and U1.1 linked with U2.1) got out of sync. This means that the flow direction changeover point is not aligned, which results in efficiency decrease. In order to solve the sync problem, an algorithm is embedded into the central unit's firmware, which periodically generates and broadcast a synchronization message. The synchronization period is set to 48 hours. Upon receive, the hub units perform a reset operation, which restarts the onboard controller of the ventilation system. The synchronization message can be generated manually or from the web-interface.

3 Results

The measurements were performed after carrying out an initial reset and providing the absolute humidity. Figures 8-9-10 show the measured temperature, RH and CO_{2eq} values in the Google spreadsheet during 12 hours of automated recording. During the measurements the heating system of the building functioned automatically, controlled with a separated device according to preset temperature values.

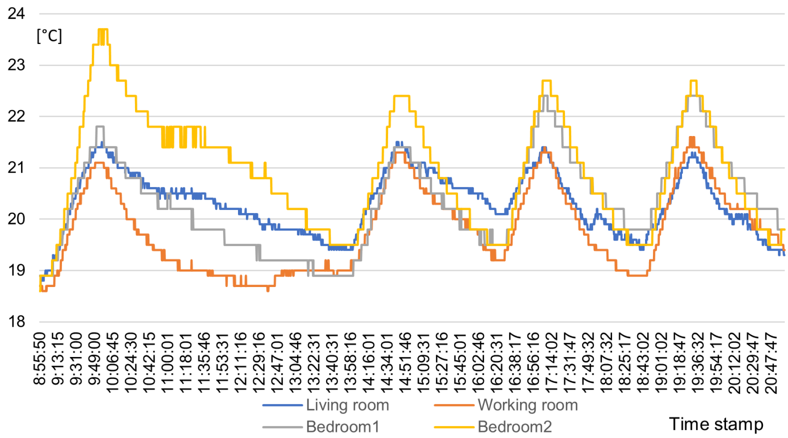

Figure 8
Variation of the temperature in the rooms

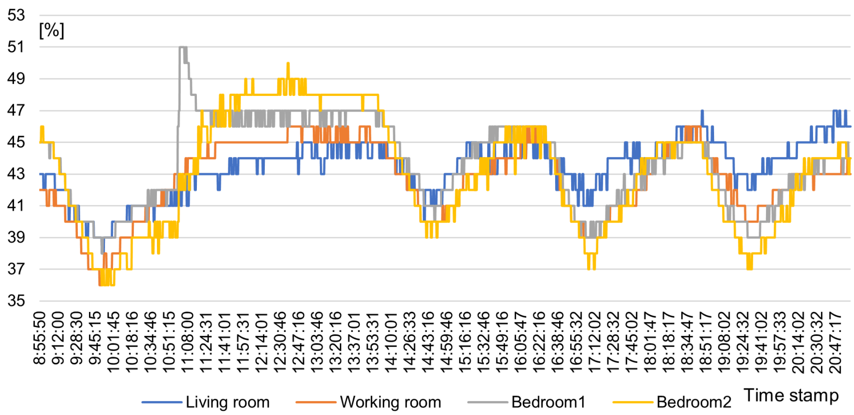

Figure 9
Variation of the relative humidity in the rooms

During the 12 hours monitoring, a 15 second sampling interval was used to display the measured values on the application live graphs and to export them in the Google spreadsheet. This interval was chosen for all three parameters (temperature, RH and CO_{2eq} levels) since they change rather slowly in real-life conditions.

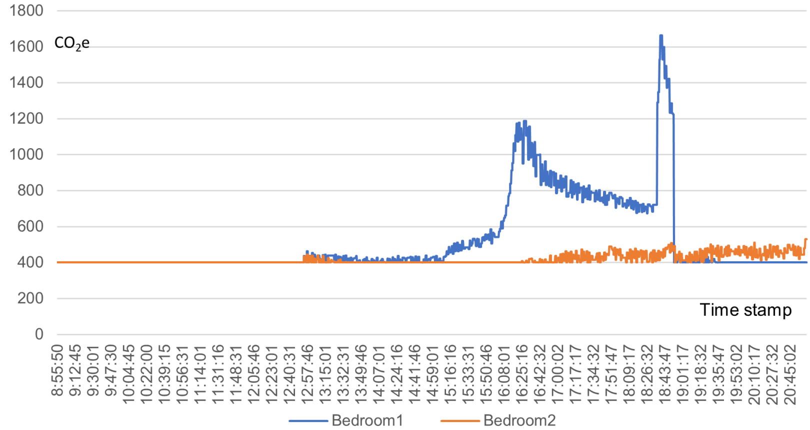

Figure 10

Variation of the CO_{2eq}

In Figure 11, an experiment can be observed about how fast the system detects and ventilates if a considerable amount of CO_2 is deployed in the room. The CO_{2eq} level in Bedroom2 was raised artificially up to around 4000 CO_{2eq} by deploying a small amount of alcohol to trigger the system. The experiment lasted until 400 CO_{2eq} baseline level was reached. The recovery to the baseline was roughly 27 minutes.

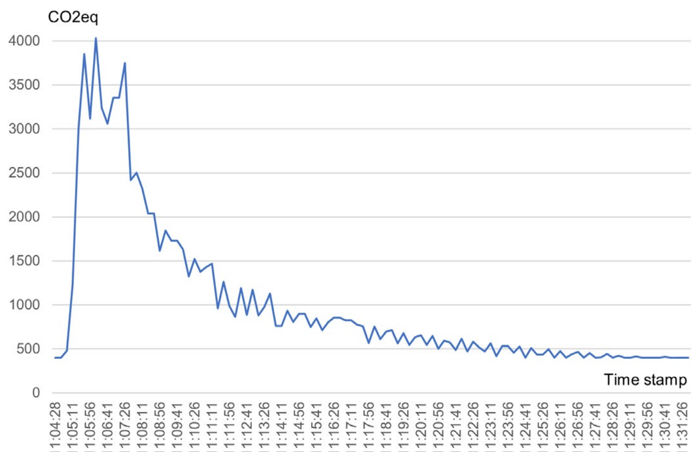

Figure 11

Variation of the CO_{2eq}

To calculate the thermal efficiency of the single units and the complete system, temperatures in the outlet of the ducts were measured using a 5 sec sampling interval (set in the HMI interface), along 100 samples. A graph depicting the variation of the temperatures in the ventilation unit's duct (at -12°C outside temperature and at ventilation speed of 2) can be seen in Figure 12.

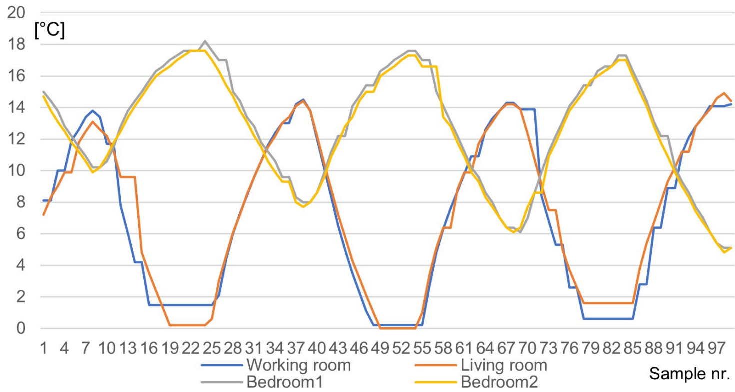

Figure 12

Variation of the temperature at the duct

Table 3 contains the individual thermal efficiencies (η) of each dMVHR unit calculated by Equation 2 and the average thermal efficiency for the complete system. As a whole ventilating cycle takes 75 sec + 75 sec = 150 sec. With a 5 sec sampling time (set for temperature measurement) it gives 30 consecutive measurements for one complete ventilating cycle. Therefore, the average temperatures for each unit, and each fan speed, can be calculated from any 30 consecutive temperatures. The speed mode was set at least 300 sec before each measurement cycle.

Table 3

Measurement and comparison of thermal efficiency

		Thermal efficiency (η %)					
T_{amb} [°C]	**Speed** [-]	**Living room**	**Working room**	**Bed-room 1**	**Bed-room 2**	**System (measured)**	**Manuf. (declared)**
+4	1	56.8	61.8	85.0	86.9	72,75	82
+4	2	61	63	78	80	70,5	74
+4	3	66	67	71	73	69,25	70
-3	1	56	71	81	88	74	82
-3	2	59	69	78	78	71	74
-3	3	45	54	80	86	66,25	70
-12	1	51	49	96	93	72,25	82
-12	2	60	58	85	82	71,25	74
-12	3	64	63	73	73	68,25	70

3 Discussion

The monitoring program displays and registers the last communicated values, which means that each measurement of the RH and CO_{2eq} are registered 4 times (60 sec / 15 sec = 4) in the Google spreadsheet. This fact is depicted in the charts similar to square functions. As the purpose of the charts from Figures 8 and 9 is to visualize the exact data structure of the database, the charts were left in their raw form.

With regard to the ability and effectivity of the system to ventilate arising CO_{2eq}, Figures 9 and 10 must be examined. It is seen that CO_{2eq} is solely measured in the bedrooms, which are habited mostly during night time. Therefore, the lowest noise level of the ventilation is required (mainly the first, or if it is necessary the second speed of the fan).

To simulate the effectivity of the automatic fan speed switch, a rapid increase of CO_{2eq} level is needed. This was carried out by contaminating Bedroom 2 with 3 ml of 70% alcohol. A small alcohol quantity in the air respresents a high-level of CO_{2eq} value, which triggers the automation algorithm rapidly to speed 3, efficiently ventilating the room. When this value decreases below 1500 CO_{2eq}, the automation system decreases the speed of the fan to speed 2, while below 1000 CO_{2eq} level, speed is decreased to speed 1.

With respect to the thermal efficiency, Figure 8 demonstrates different temperatures detected at the two floors, which lead to dissimilar thermal efficiency of the units on the first floor and the ground floor.

The explanation of this phenomenon can be derived from the fact that even when ventilation stops, a constant air flow is maintained between the two floors via the montage holes. As outside temperature starts droping, internal airflow begins to increase. Due this phenomenon, the volumetric airflow values of the units, are altered significantly.

This can be seen clearly by the temperature variations registered at -12°C outside temperatures. There is 20-23% difference in efficiency between speed 1 and speed 3, while at +4°C the difference in efficiency is only 14%.

If we consider all units together as a system, and we compare the efficiency with the one, provided by the manufacturer, then the results are in close accordance. For example, in case of +4°C, we have obtained the declared efficiancy values from the manufacturer. Althought at speed 1 the overall difference in thermal efficiency is approximately 10%, in case of speed 2 and 3 it reduces to 4% and 1%.

The small difference in the measured data and the manufacturers's data is due to the face that the ventilation setup of the examined building is in no case a laboratory setup. Difference can be originated to many factors such as:

temperature dependent airflow between the building floor levels, imperfect sealing of the windows.

Nevertheless, the automation of the heat recovery ventilation system works as it was intended and it is also capable of evaluating a true thermal efficiency of a dMVHR system in real-life (not perfectly sealed) environment.

In conclusion, this particular effect of the SHT21 sensor is important in case of the rapidly changing temperature measurements around 0°C, but in case of a home automation, where slower changes are being monitored, this attribute does not influence the system incorrectly.

Limitations

Airflow temperature and humidity measurement with the SHT21 sensor presented some difficulties at low temperatures. As it can be seen in Figure 10, the measured temperature values freeze for 20-40 seconds, around the 0°C, when the flow direction at the ground-floor unit's changes. A plausible explanation is that due to cold airstream the sensor temperature also drops, and when the airflow changes, the inside air humidity content precipitates on the temperature sensor.

This results in altering some measured values to constants, but only around 0°C, and for a short time.

Conclusions

The proposed dMHVR system proved to be effective and stable to maintain the three major IAQ parameters (temperature, air humidity and CO_{2eq}) in the examined rooms of the building. In addition, the online monitoring system allows the user to intervene and manually override the control process. It must be mentioned that data during the control can be downloaded and stored. The system also has the ability to provide data about its thermal efficiency, with regard to single units or the complete system. It could be concluded that the measured efficiancy and the standard efficiency (provided by the manufacturer) are in good correlation with each other.

Acknowledgement

No financial support has been provided to the authors.

References

[1] Zender-Świercz, E.: A Review of Heat Recovery in Ventilation. Energies 2021, 14, 1759, pp. 1-23, https://doi.org/10.3390/en14061759

[2] Pekdogan, T.; Tokuç, A.; Ezan, M. A.; Başaran, T.: Experimental investigation of a decentralized heat recovery ventilation system. Journal of Building Engineering, Volume 35, 2021, 102009, pp. 1-13, https://doi.org/10.1016/j.jobe.2020.102009

[3] Merzkirch, A.; Maas, S.; cholzen, F.; Waldmann, D.: Field tests of centralized and decentralized ventilation units in resi-dential buildings – Specific fan power, heat recovery efficiency, shortcuts and volume flow unbalances. Energy and Buildings, Volume 116, 2016, pp. 376-383, https://doi.org/10.1016/j.enbuild.2015.12.008

[4] Zemitis, J.; Bogdanovics, R. Heat recovery efficiency of local decentralized ventilation devices. Magazin of Cicile Engineering, 2020, Issue 2(94), pp. 120-128, DOI: 10.18720/MCE.94.10

[5] Carbonare, N.; Fugmann, H.; Asadov, N.; Pflug, T.; Schnabel, L.; Bongs, C.: Simulation and Measurement of Energetic Performance in Decentralized Regenerative Ventilation Systems. Energies 2020, 13, 6010, pp. 1-25, https://doi.org/10.3390/en13226010

[6] Ferreira Silva, M.; Maas, S.; Artur de Souza, H.; Pinto Gomes, A.: Post-occupancy evaluation of residential buildings in Luxembourg with centralized and decentralized ventilation systems, focusing on indoor air quality (IAQ). Assessment by questionnaires and physical measurements, Energy and Buildings, Volume 148, 2017, pp. 119-127, https://doi.org/10.1016/j.enbuild.2017.04.049

[7] Genc, A. M.; Karadeniz, Z. H.; Ekren, O.; Toksoy, M. A Novel Spherical Packed Bed Application on Decentralized Heat Recovery Ventilation Units, E3S Web of Conferences 111(2019) 01012, Clima 2019, pp. 1-8, Bucharest, Romania, 26-29 May 2019, https://doi.org/10.1051/e3sconf/201911101012

[8] Davidsson, H.; Johansson, D.; Chowdary, S. K.: Decentralized ventilation unit for window frame integration, Proceedings of IOP Conf. Ser.: Earth Environ. Sci. 1085 (2022) 012030, pp. 1-8, Hague, Netherlands, October 2022, doi:10.1088/1755-1315/1085/1/012030

[9] Quantum HR. Decentralized Heat Recovery Unit. Available online: https://www.aerauliqa.com/pdf/datasheet/Quantum_HR.pdf (accessed on 08 February 2023)

[10] Vinnarasi, A.; Sangeetha, M.: Comfort Cognitive IoT for Efficient Monitoring and Predictive in Building Management Systems, Proceedings of Sixth International Conference on Wireless Communications, Signal Processing and Networking (WiSPNET), Chennai, India, 25-27 March 2021, pp. 345-349, DOI: 10.1109/WiSPNET51692.2021.9419408

[11] Stolojescu-Crisan, C.; Crisan, C.; Butunoi, B.-P.: An IoT-Based Smart Home Automation System. Sensors 2021, 21, 3784, pp.1-23, https://doi.org/10.3390/s21113784

[12] Khan, M.A. et.al.: Smart Android Based Home Automation System Using Internet of Things (IoT). Sustainability 2022, 14, 10717, pp. 1-17, https://doi.org/10.3390/su141710717

[13] Elkholy, M.H.; Senjyu, T.; Lotfy, M.E.; Elgarhy, A.; Ali, N.S.; Gaafar, T.S.: Design and Implementation of a Real-Time Smart Home Management System Considering Energy Saving. Sustainability 2022, 14, 13840, pp. 1-22, https://doi.org/10.3390/su142113840

[14] Khalil, M.; Esseghir M.; Merghem-Boulahia, L.: Applying IoT and Data Analytics to Thermal Comfort: A Review, Machine Intelligence and Data Analytics for Sustainable Future Smart Cities, Studies in Computational Intelligence 971, Ghosh, U., Maleh, Y., Alazab., M, Pathan, A-S. K., Eds.; Springer: Berlin/Heidelberg, Germany, 2021, pp. 171–198

[15] Zang, M.; Xing, Z.; Tan, Y.: IoT-based personal thermal comfort control for livable environment. International Journal of Distributed Sensor Networks. 2019; 15(7), doi:10.1177/1550147719865506

[16] Laftchiev, E.; Nikovski, D.: An IoT system to estimate personal thermal comfort, 2016 IEEE 3rd World Forum on Internet of Things (WF-IoT), Reston, VA, USA, 2016, pp. 672-677, doi: 10.1109/WF-IoT.2016.7845401

[17] Minarčík, P.; Procházka, H.; Gulan, M.: Advanced Supervision of Smart Buildings Using a Novel Open-Source Control Platform. Sensors 2021, 21(1), 160, pp. 1-21, https://doi.org/10.3390/s21010160

[18] Saikat Islam Khan1 et. al.: IoT and Wireless Sensor Networking-based Effluent Treatment Plant Monitoring System, Acta Polytechnica Hungarica, Volume 18, Issue 10, 2021, pp. 205 – 224, DOI: 10.12700/APH.18.10.2021.10.11

[19] Datasheet SHT21. Available online: https://sensirion.com/media/documents/120BBE4C/63500094/Sensirion_Datasheet_Humidity_Sensor_SHT21.pdf (accessed on 08 June 2022)

[20] Datasheet SGP30, Available online: https://sensirion.com/media/documents/984E0DD5/61644B8B/Sensirion_Gas_Sensors_Datasheet_SGP30.pdf (accessed on 08 June 2022)

[21] Martínez-Parrales, R; Téllez-Anguiano, A.C.: Vibration-based Fault Detection System with IoT Capabilities for a Conveyor Machine, Acta Polytechnica Hungarica, Volume 19, Issue 9, 2022, pp. 7 – 24, DOI: 10.12700/APH.19.9.2022.9.1

[22] Ferencz, K.; Domokos, J.; Kovács, L.: Cloud Integration of Industrial IoT Systems. Architecture, Security Aspects and Sample Implementations, Acta Polytechnica Hungarica, Volume 21, Issue 4, 2024, pp. 7 – 28, DOI: 10.12700/APH.21.4.2024.4.1